Am J Transl Res 2026;18(1):190-206
www.ajtr.org /ISSN:1943-8141/AJTR0169020

Original Article

Tanshinone IIA prevents septicemia acute kidney injury via regulating the DUSP10/JNK/P38/NLRP3 pathway

Dan Wen, Qing Deng, Ying Zeng, Longzhu Li, Xin Yang, Qinkai Chen, Yan Yan, Jinlei Lv

Department of Nephrology, The 1st Affiliated Hospital, Jiangxi Medical College, Nanchang University, Institute of Molecular Immunology for Kidney Disease of Nanchang University, Nanchang 330000, Jiangxi, China

Received September 26, 2025; Accepted December 6, 2025; Epub January 15, 2026; Published January 30, 2026

Abstract: Objective: To investigate the protective effects and underlying mechanisms of tanshinone IIA in preventing septicemia acute kidney injury (SA-AKI). Methods: Mice were pretreated with tanshinone IIA via intraperitoneal injection, followed by lipopolysaccharide (LPS) administration to induce SA-AKI. Hematoxylin-eosin (HE) staining was used to assess renal tissue injury to confirm successful model establishment. In vitro, HK2 cells were treated with LPS and/or tanshinone IIA. Differentially expressed genes (DEGs) between the LPS and tanshinone IIA + LPS groups were identified via high-throughput sequencing. qPCR was performed to validate mRNA expression of key DEGs. Protein expression in mouse kidney and HK2 cells was analyzed using immunohistochemistry and western blot. Results: Mice in the SA-AKI model demonstrated severe renal damage, with elevated levels of serum creatinine and urea nitrogen, as well as increased apoptosis and glycogen accumulation. Tanshinone IIA pretreatment significantly alleviated these pathological changes. Flow cytometry confirmed that LPS induced HK2 cell apoptosis, which was attenuated by tanshinone IIA. Transcriptomic analysis revealed 121 upregulated and 65 downregulated genes. Western blot showed that LPS increased JNK, p38, NLRP3 and Caspase-1 expression, and decreased DUSP10 and ALDH2 expression, while tanshinone IIA pretreatment reversed these effects. Similarly, immunohistochemistry and western blot analyses demonstrated elevated contents of KIM-1, NLRP3, JNK and Caspase-1, and reduced DUSP10 and ALDH2 in SA-AKI mice. Conclusion: Tanshinone IIA exerts a protective effect against SA-AKI by mitigating inflammation and apoptosis. Mechanistically, these effects appear to be mediated through DUSP10 and modulation of the JNK/P38/NLRP3 pathway. These findings suggest that tanshinone IIA might be a potential therapeutic strategy for SA-AKI.

Keywords: Sepsis, acute kidney injury, tanshinone IIA, DUSP10, NLRP3

Introduction

Sepsis is a systemic inflammatory response syndrome caused by infection [1] and is frequently accompanied by acute kidney injury (AKI). AKI is a clinical syndrome characterized by a sudden (within 1-7 days) and sustained (>24 h) decline in renal function, manifested by elevated blood creatinine and urea nitrogen, disrupted water electrolyte and acid-base balance, and decreased urine output [2]. Septicemia acute kidney injury (SA-AKI) is a common complication in critically ill patients and represents an early marker of sepsis progression. About 50% of septic shock patients develop AKI before arriving at the emergency department [3]. The mortality of SA-AKI remains high, which is about 8 times higher than that of sepsis patients without AKI [4]. However, the one-year mortality rate is comparable between patients who recover from SA-AKI and those who never develop AKI, indicating that the pathophysiological process of SA-AKI may be reversible [5]. SA-AKI has an impact on multiple organs, increasing the risk of patient mortality and long-term complications. Some survivors may develop secondary cerebrovascular disease, while others may even progress to chronic kidney disease [6-8]. According to statistics, nearly 19 million individuals develop sepsis worldwide each year, and approximately 11 million of them experience SA-AKI [9]. The medical expenses spent on SA-AKI each year are enormous, but the results are minimal. Therefore,

https://doi.org/10.62347/VJEI5652

investigating the pathogenesis of SA-AKI and identifying effective preventive strategies are of great significance.

The pathogenesis of SA-AKI is complex, involving endothelial cell dysfunction, inflammatory response, and structural and functional damage to glomeruli and tubules [10]. Sepsis-induced inflammatory response plays an important role in the occurrence of SA-AKI [11]. During sepsis, large quantities of inflammatory mediators are released and bind to T cell like receptors and undergo signaling cascades to promote the release of inflammatory factors [12]. In recent years, the innate immune receptor nucleotide-binding oligomerization domain-like receptor protein 3 (NLRP3) inflammasome has been recognized as a key factor in the SA-AKI inflammatory response. NLRP3 inflammasomes can promote the activation of cysteine aspartate specific protein 1 (Caspase-1) and interleukin maturation, exacerbating inflammatory response damage to cells [13, 14]. In addition, in renal tubular epithelial cells, pathogen-associated molecular patterns (PAMPs) and damage-associated molecular patterns (DAMPs) bind with innate immune receptor toll like receptors (TLRs) to trigger downstream signaling cascades, activate NF-κB, upregulate inflammatory cytokine gene expression, trigger inflammatory reactions, increase oxidative stress; all of which results in serious damage to renal tubular epithelial cells by ROS (Reactive Oxygen Species) [15, 16]. Therefore, preventing these factors' expression, which are related to the inflammatory response, may be targets for SA-AKI therapy.

Danshen, a widely used herb in traditional China medicine (TCM), is known for its functions of clearing heat and toxins, promoting blood circulation, and removing blood stasis [17, 18]. It is well known that Danshen has good therapeutic effects on tumors, cardiovascular diseases, and renal fibrosis [19]. Tanshinone IIA, a major lipid-soluble bioactive component extracted from *Salvia miltiorrhiza*, has been shown to protect cells and tissues by reducing toxicity, regulating cell proliferation and apoptosis, as well as inhibiting inflammatory responses and oxidative stress [20, 21]. Previous studies have also demonstrated that tanshinone IIA ameliorates kidney injury induced by hyperuricemia and diabetes [22, 23], and provides protective effects on sepsis-induced AKI in rats [24]. It is reported that tanshinone IIA treatment increases the expression of proliferating cell nuclear antigen, reduces the infiltration of inflammatory cells and the expression of chemokines, promotes kidney repair after AKI, and inhibits the local inflammatory response of the damaged kidney [25]. Although tanshinone IIA has therapeutic effects on SA-AKI, the molecular mechanism underlying its function in SA-AKI is still unclear. The purpose of this study is to systematically investigate the effects of tanshinone IIA on SA-AKI and to elucidate its specific molecular mechanisms, particularly focusing on its regulatory role in inflammation and apoptosis through the DUSP10/JNK/p38/NLRP3 signaling pathway.

Materials and methods

Experimental animals

A total of 27 male C57BL/6J mice (7 weeks old) were purchased from Beijing Huafukang Biotechnology Co., Ltd. (license number: SCXK (Jing) 2019-0010). At the end of the experiment, all mice were humanely euthanized in accordance with institutional ethical guidelines. Euthanasia was performed by intraperitoneal injection of an overdose of pentobarbital sodium (150 mg/kg body weight), and death was confirmed by the absence of breathing and heartbeat, as well as loss of corneal reflex for at least one minute. All procedures were conducted to minimize animal suffering and distress.

All animal experiments were conducted in accordance with the guidelines of the Institutional Animal Care and Use Committee (IACUC) and were approved by the Ethics Committee of the First Affiliated Hospital, Jiangxi Medical College, Nanchang University.

Experimental cells

Human renal cortex proximal tubule epithelial cells (HK2) were sourced from iCell Bioscience Inc. (iCell-h096; Shanghai).

Experimental reagents

Lipopolysaccharide (LPS) (1001164401, Sigma); Tanshinone IIA (131523, Targeted MOl); Serum creatinine (CREA) test kit (70127,

Shandong Boke Biotech); Urea nitrogen (UREA) Kit (70124, Shandong Boke Biotech); Hematoxylin dye solution (ZLI-9610, Zhongshang Jinqiao); Eosin staining solution (G1100, Solarbio); blue dyeing liquid (G1040, Servicebio); TUNEL detection kit (red) (C1090, Beyotime); RIPA cell lysate (C1053, Beijing Pulilai Gene Technology Co., Ltd.); BCA Protein Assay Kit (E-BC-K318-M, Elabscience); Ultra-sensitive luminescent liquid (RJ239676, Thermo Fisher Scientific); Internal reference primary antibody: Mouse Anti GAPDH (HC301, TransGen Biotech); Secondary antibody: HRP-conjugated Goat Anti Mouse IgG (H+L) (GB23301, Servicebio); Rabbit Anti ALDH2 (ab108306, Abcam); Rabbit Anti Caspase-1 (YT5743, ImmunoWay); Rabbit Anti JNK (66210-1-lg, Proteintech); Rabbit Anti NLRP3 (A00034-2, Boster); Rabbit Anti p38 (14064-1-AP, Proteintech); Rabbit Anti DUSP10 (30493-1-AP, Proteintech); HRP-conjugated Goat Anti-Rabbit IgG (H+L) (GB23303, Servicebio); DAB staining kit (CW0125M, CWBIO); Rabbit anti-KIM-1 antibody (NOVUS, NBP1-76701SS); CCK-8 detection kit (KGA9310-500, KeyGEN); Annexin V-FITC/PI Apoptosis Kit (AP101-100-kit, MULTI SCIENCES); Trizon Reagent (CW-0580S, CWBIO); Glycogen PAS staining reagent (G1281, Solarbio).

Experimental instruments

Fully automatic biochemical analyzer (BK-600, Shandong Boke); Microscope (CX43, Olympus); Multi-functional enzyme-linked immunosorbent assay reader (SuperMax3100, Shanghai Flash Spectrum Biological Technology Co., Ltd.); Protein vertical electrophoresis instrument (DYY-6C, Beijing Liuyi Instrument Factory); Fully automatic chemiluminescence image analysis system (Tanon-5200, Shanghai Tianneng Technology Co., Ltd.); CO_2 incubator (BPN-80CW, Shanghai Yiheng Scientific Instrument Co., Ltd.); Inverted fluorescence microscope (MF53 Guangzhou Mingmei Optoelectronics Co., Ltd.); UV spectrophotometer (NP80, NanoPhotometer); Electrophoretic apparatus (DYY-8C, Beijing Liuyi Biotechnology Co., Ltd.); Ordinary PCR amplification instrument (TC-EA, Hangzhou Bori Technology Co., Ltd.); Fluorescent PCR instrument (CFX Connect™ Real Time, BioRad Life Medical Products (Shanghai) Co., Ltd.); Ultra high sensitivity chemiluminescence imaging system (ChemiDocTM XRS+, BioRad Life Medical Products (Shanghai) Co., Ltd.).

Animal feeding and handling

The animal experiments were approved by the Institutional Animal Care and Use Committee of The First Affiliated Hospital of Nanchang University (CDYFY-IACUC-202304QR058).

The mice were house at 20-26°C with a humidity of 40%-70%, with ad libtum access to drinking water. After adaptive feeding, the mice were randomly divided into four groups: Control group (n=7), Model group (n=7), Control + Tanshinone IIA group (n=6), and Model + Tanshinone IIA group (n=7). The mice were subjected to intraperitoneal injection of 10 mL/kg of tanshinone IIA (5 mg/mL, Tanshinone dissolved in 0.02% DMSO physiological saline) in the Control + Tanshinone IIA group and Model + Tanshinone IIA group [26], and intraperitoneal injection of physiological saline containing 0.02% DMSO (Dimethyl sulfoxide) in the control group and model group. Three hours later, the model group and model + Tanshinone IIA group were intraperitoneally injected with 10 mL/kg of LPS (LPS concentration: 1.5 mg/mL), while the control group and control + Tanshinone IIA group were intraperitoneally injected with an equal amount of physiological saline. Twenty-four hours after the intraperitoneal injection, blood was taken for biochemical testing, and the kidney was taken for subsequent experiments.

Fully automatic biochemical analyzer detection

The blood samples from the mice were obtained and centrifuged at 3,500 rpm for 10 min. The supernatant was collected, and the serum CREA kit and UREA kit were used to detect the levels of serum creatinine and urea nitrogen.

Hematoxylin-eosin (HE) staining

Kidney tissues of each group of mice were fixed and dehydrated with 70%, 80%, and 90% ethanol solutions. The tissues were cleared in xylene I and II (15 min each) until fully transparent and subsequently immersed in a xylene-paraffin mixture for 15 min. The tissues were then incubated in paraffin I and paraffin II for 50-60 min each before paraffin embedding and sectioning. Paraffin sections were baked, deparaffinized, and rehydrated through graded ethanol to distilled water. The slices were stained with hematoxylin for 3 min, differentiated in hydro-

Table 1. Antibodies and dilutions

Antibody name	Dilutions
Mouse Anti-GAPDH (HC301, TransGen Biotech)	1:2000
HRP conjugated Goat Anti-Mouse IgG (GB23301, Servicebio)	1:2000
Rabbit Anti ALDH2 (ab108306, Abcam)	1:1000
Rabbit Anti Caspase-1 (YT5743, ImmunoWay)	1:1000
Rabbit Anti JNK (66210-1-Ig, Proteintech)	1:1000
Rabbit Anti NLRP3 (A00034-2, boster)	1:1000
Rabbit Anti p38 (14064-1-AP, Proteintech)	1:1000
Rabbit Anti DUSP10 (30493-1-AP, Proteintech)	1:1000
HRP conjugated Goat Anti-Rabbit IgG (GB23303, Servicebio)	1:2000

Notes: GAPDH, glyceraldehyde-3-phosphate dehydrogenase; ALDH2, aldehyde dehydrogenase 2; KIM-1, kidney injury molecule 1; Caspase-1, cysteine aspartate specific protein 1; JNK, c-Jun N-terminal kinase; NLRP3, nucleotide-binding oligomerization domain-like receptor protein 3; DUSP10, dual specificity phosphatase 10.

chloric acid ethanol for 15 s, rinsed briefly in water, and blued for 15 s. After rinsing with running water, the sections were counterstained with eosin for 3 min, washed, dehydrated, cleared, and mounted. Stained sections were observed under a microscope.

Terminal deoxynucleotidyl transferase-mediated dUTP Nick End Labeling (TUNEL) staining

Kidney tissues were fixed, sliced paraffin-embedded, sectioned, baked, dewaxed, and rehydrated through a graded ethanol series. Antigen retrieval was performed using Proteinase K working solution, followed by three washes with PBS. A sufficient amount of TUNEL reaction solution was added to each section and incubated in the dark according to the manufacturer's instructions. After washing, the sections were counterstained with DAPI (4',6-Diamidino-2'-phenylindole) for 5 min. Finally, the slides were mounted with an anti-fluorescence quenching mounting medium, and apoptotic cells were observed under a fluorescence microscope.

Western blot detection

The total protein of the tissue or cells were centrifuged to obtain the supernatant. The total protein was quantified using the Bicinchoninic Acid Assay (BCA) protein quantification kit. Equal amounts of protein were denatured and separated by sodium dodecyl sulfate-gel electrophoresis (SDS-PAGE), followed by electrotransfer onto polyvinylidene fluoride (PVDF) membranes at a constant current of 300 mA. After blocking with skim milk powder, the primary antibody was added for incubation overnight at 4°C, followed by incubation with the secondary antibody at room temperature the next day. Protein bands were visualized using an enhanced chemiluminescence (ECL) substrate and imaged using an ultra-sensitive chemiluminescence detection system. The antibodies used and their corresponding dilution ratios are shown in **Table 1**.

Immunohistochemical detection

Kidney tissues were fixed, embedded in paraffin, and sectioned. After baking, the sections were deparaffinized in xylene and rehydrated through a graded ethanol series. The slices were heated in antigen retrieval buffer, followed by incubation with 3% hydrogen peroxide to quench endogenous peroxidase activity. The slices were permeabilized with 0.5% TritonX-100, blocked with 5% BSA, and incubated with rabbit anti-Acetaldehyde dehydrogenase 2 (ALDH2) antibody (Affinity, DF6358, 1/100), rabbit anti-Dual specificity phosphatase 10 (DUSP10) antibody (Affinity, DF4694, 1/100), rabbit anti-Kidney injury molecule 1 (KIM-1) antibody (NOVUS, NBP1-76701SS, 1/100), and rabbit anti-Nucleotide-binding oligomerization domain-like receptor protein 3 (NLRP3) antibody (BIOSS, BS-10021R, 1/100) overnight at 4°C. The next day, the sections were incubated with goat anti rabbit IgG (H+L) (1:100) labeled with horseradish enzyme at 37°C for 30 min. Signal detection was performed using DAB staining for 3-5 min, and hematoxylin counterstaining for 3 min. After differentiation with acid alcohol and bluing, the sections were dehydrated through graded ethanol, cleared in xylene, mounted with neutral resin, and examined under a light microscope.

Cell culture and treatment

HK2 cells were cultured in a complete DF12 medium at 37°C in a 5% CO_2 incubator. Different concentrations of LPS (0, 5, 10, 20, 40, 80, 160 μg/mL) were added to HK2 cells to establish an inflammatory model, and cell viability was detected by CCK-8 to determine the optimal concentration of LPS treatment. Pre-

treatment was performed by adding different concentrations of tanshinone (0, 2.5, 5, 10, 20, 40, 80 μM) to HK2 cells. After 30 min, the determined concentration of LPS was added, and cell viability was detected by CCK-8 assay 24 h later. HK2 cells were seeded and grouped into a HK2 cell group, HK2 cells + LPS group, HK2 cells + tanshinone group, and HK2 cells + tanshinone + LPS group.

CCK-8 testing

After treatment, the culture medium in each well of a 96-well plate was replaced with 100 μL of fresh medium. Then, 10 μL of CCK-8 reagent was added to each well, followed by incubation at 37°C for 2 h. The absorbance of each well was detected at 450 nm using a microplate reader.

Flow cytometry detection of cell apoptosis

Approximately 1 × 10^6 cells from each group were collected and washed twice with PBS at 1,500 rpm for 3 min. The cells were resuspended in 300 μL of pre-cooled 1 × Annexin V-FITC binding solution. Next, 5 μL of Annexin V-FITC (AP101-100-kit, MULTI SCIENCE) and 10 μL of PI were added to each well. After gentle mixing, the samples were incubated at room temperature in the dark for 10 min and subsequently analyzed using a flow cytometer.

High-throughput sequencing

Cells from HK2 cells + LPS group and HK2 cells + tanshinone + LPS group were collected for mRNA high-throughput sequencing. Total RNA was extracted and subjected to quality assessment before library construction. The sequencing was performed on the Illumina platform. After raw data quality control, adaptor trimming, and removal of low-quality reads, high-quality clean reads were obtained. The reads were aligned to the reference genome, and gene expression levels were quantified, obtaining differentially expressed genes (DEGs).

Functional enrichment analyses, including Gene Ontology (GO), Kyoto Encyclopedia of Genes and Genomes (KEGG) pathway analysis, Reactome pathway enrichment, and Disease Ontology (DO) enrichment, were conducted to explore the biological functions and signaling pathways associated with the DEGs.

Periodic acid Schiff (PAS) staining

Mouse kidney tissues were fixed, paraffin-embedded, and sectioned. The paraffin sections were dried in a drying oven, deparaffinized and rehydrated through graded xylene and ethanol, then oxidized for 15 min, washed with water, and incubated with Schiff reagent for 10 min at room temperature. After washing with sodium sulfite solution and water, the sections were counterstained with hematoxylin, rinsed, air dried, and observed under a microscope.

Real time fluorescence quantitative PCR (qPCR) detection

Total RNA was extracted from tissues or cells using Trizon reagent. mRNA was extracted using RNA ultrapure extraction kit. mRNA concentration and purity were measured using a UV visible spectrophotometer (OD260/OD280). cDNA was synthesized using a RNA reverse transcription kit, and fluorescence quantitative PCR was performed using a fluorescence PCR instrument. The reaction steps were as follows: pre-denaturation at 95°C for 10 min, 40 cycles of denaturation at 95°C for 10 sec, annealing at 58°C for 30 sec, and extend at 72°C for 30 sec. β-actin was used as an internal reference, and the relative gene expression levels were calculated using the $2^{-\Delta\Delta Ct}$ method. The primer sequences are shown in **Table 2** (synthesized by Anhui General Biotechnology Co., Ltd.).

Statistical analysis

All results were expressed as mean ± standard deviation (x ± sd). The statistical analysis and plotting were conducted using Graphpad Prism 8.0 software. Comparisons between two groups were performed using t-test, and among multiple groups were performed using ANOVA. $P<0.05$ was considered as a significant difference.

Results

Effects of tanshinone IIA on the characterization of SA-AKI mice

To explore the effects of tanshinone IIA on SA-AKI mice, the levels of serum creatinine and urea nitrogen were measured, and renal injury was observed by HE. As shown in **Figure 1A**, **1B**, compared with the Control group, the

Table 2. Primer sequences

Primer name	Primer sequences (5'-3')	Product length (bp)	Annealing temperature (°C)
GAPDH F	TGACTTCAACAGCGACACCCA	121	58.0
GAPDH R	CACCCTGTTGCTGTAGCCAAA		
DUSP10 F	TCGGCTACGTCATCAACGTC	155	58.0
DUSP10 R	CTGGTGAGCTTCCTCAATGAAC		
HSPA1A F	CAGAACAAGCGAGCCGTGAG	172	58.0
HSPA1A R	TTCGGAACAGGTCGGAGCA		
DDIT3 F	GAACCAGCAGAGGTCACAAGC	290	58.0
DDIT3 R	TTCACCATTCGGTCAATCAGA		
GADD45A F	GTGCTGGTGACGAATCCACA	89	58.0
GADD45A R	TCCATGTAGCGACTTTCCCG		
EFNA1 F	AACAGTTCAAATCCCAAGTTCCG	152	58.0
EFNA1 R	TCCTCATGCTCCACCAGGTA		
EGLN3 F	GGACAACCCCAACGGTGAT	82	58.0
EGLN3 R	CCCACCATGTAGCTTGGCAT		

Notes: GAPDH, glyceraldehyde-3-phosphate dehydrogenase; DUSP10, dual specificity phosphatase 10; HSPA1A, Heat shock protein family A member 1A; DDIT3, Damage-inducible transcript 3; GADD45A, Growth arrest and DNA damage-45A; EFNA1, Ephrin A; EGLN3, Egl-9 Family Hypoxia Inducible Factor 3.

Model group showed a significant increase in serum creatinine and urea nitrogen levels, which were obviously relieved by Tanshinone IIA treatment. According to HE staining results (**Figure 1C**), the kidney structure of mice in the Control group was clear with no obvious damage, while the mice in the Model group showed swelling, vacuolization, and degeneration of renal tubular epithelial cells, confirming the successful construction of the AKI model. The mice in the Model + Tanshinone IIA group showed less renal damage compared with the Model group. The PAS staining results (**Figure 1D**) showed that there was less glycogen deposition in the Control group and the Control + Tanshinone IIA group, while the Model group showed an increase in glycogen deposition, which was reduced in the Model + Tanshinone IIA group. As shown in **Figure 1E**, TUNEL staining showed that compared with the Control group, cell apoptosis in the Model group was significantly increased, which was also suppressed in the Model + Tanshinone IIA group, confirming that Tanshinone IIA can reduce cell apoptosis caused by LPS-induced AKI.

Effect of tanshinone IIA on apoptosis of LPS-stimulated HK2 cells

CCK-8 assay was used to determine the optimal LPS concentration for treating HK2 cells. As shown in **Figure 2A**, compared with the "0 μg/mL" group, the viability of HK2 cells was significantly decreased at 5 μg/mL LPS for 24 h, which was further decreased as LPS concentration increased, and 10 μg/mL was selected for subsequent experiments. The optimal tanshinone IIA concentration was also determined. As shown in **Figure 2B**, compared with the Control group, LPS significantly decreased cell viability, while pre-treatment with 5, 10, and 20 μM Tanshinone IIA significantly increased cell viability compared with the LPS group, with 10 μM Tanshinone IIA demonstrated the most significant increase. Therefore, 10 μM Tanshinone IIA was selected for subsequent experiment.

As shown in **Figure 2C**, **2D**, flow cytometry showed that, compared with the Control group, the LPS group showed a significant increase in cell apoptosis, which was obviously alleviated in the Mod + Tanshinone IIA group, indicating that Tanshinone IIA can reduce LPS-induced cell apoptosis.

Prediction of tanshinone IIA targets in AKI using network pharmacology

The chemical structure of Tanshinone IIA obtained from PubChem was imported into the SwissTargetPrediction database identify potential pharmacological targets. A total of 43 potential active targets were identified with probability greater than 0. AKI-related disease targets were obtained from the GeneCards database, yielding 8394 targets with a relevance score greater than 1.

Using the Venny 2.1.0 online platform, 35 intersecting targets of Tanshinone IIA and AKI were obtained, as shown in **Figure 3A**. A protein-protein interaction (PPI) network was constructed using the String database. Network visualization and topological analysis were performed using Cytoscape 3.9.1, and key hub genes were screened with the cytoHubba plug-in (**Figure 3B**, **3C**). Based on four centrality algorithms (Degree, Betweenness, MCC, and DMNC), top 15 targets from each method were identified.

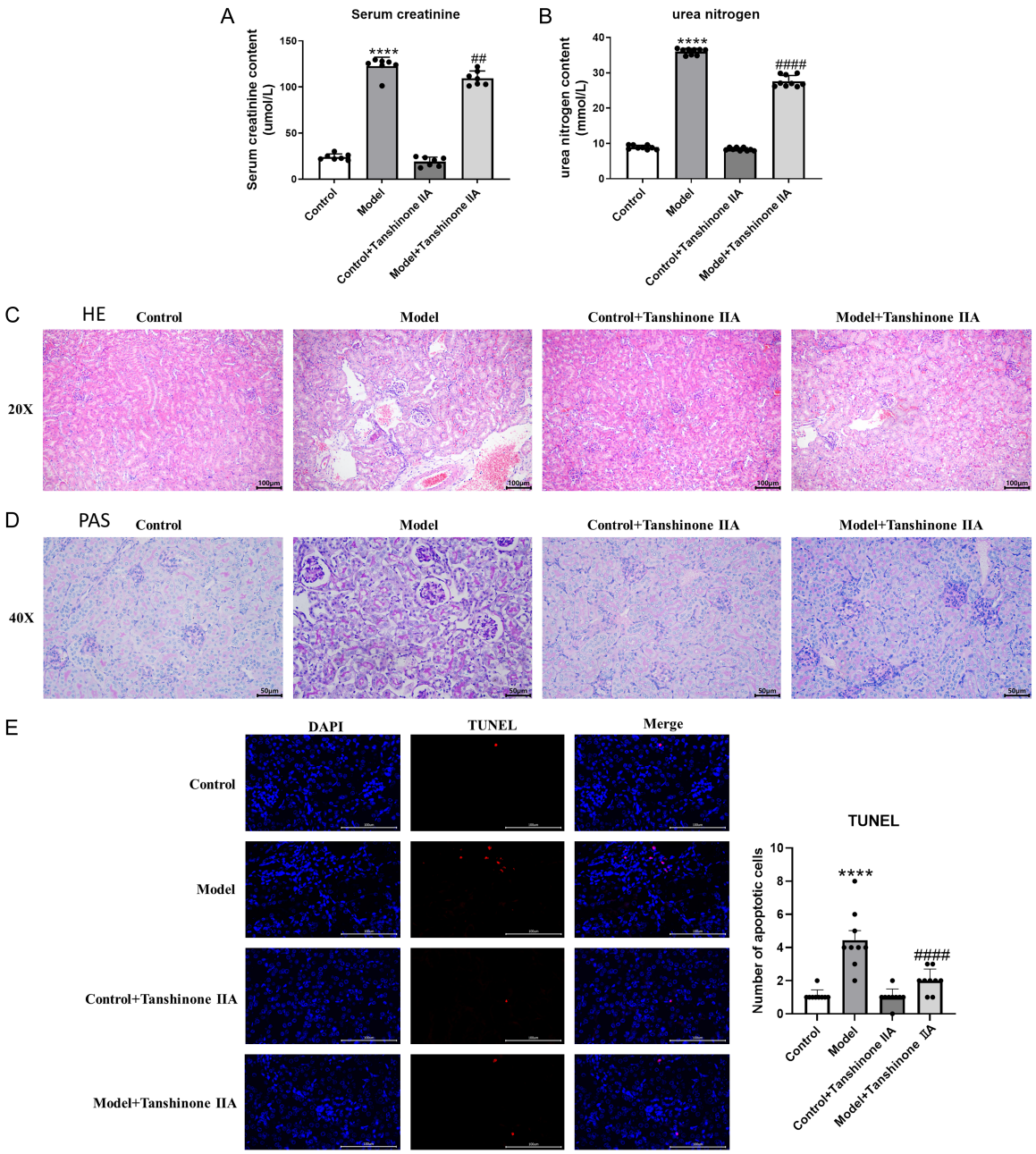

Figure 1. Tanshinone IIA treatment ameliorates mice renal function and renal tubule pathological injury and cell apoptosis induced by LPS. A, B. Results of mouse serum creatinine and urea nitrogen detected by biochemistry analyzer (compared with the Control group, ****P<0.0001; Compared with the Model group, ##P<0.01, ####P<0.0001; n=3); C. Hematoxylin-eosin staining results of mouse kidney (n=3); D. Periodic acid Schiff staining results of mouse kidney (n=3); E. TUNEL staining results of mouse kidney (compared with the Control group, ****P<0.0001; Compared with the Model group, ####P<0.0001; n=3).

Integrating these results yielded 11 core hub targets: Androgen receptor (AR), Progesterone receptor (PGR), Cell division cycle 25A (CDC25A), Cell division cycle 25B (CDC25B), Protein tyrosine phosphatase receptor type C (PTPRC), Cytochrome P450 family 19 subfamily A member 1 Gene (CYP19A1), Protein Tyrosine Phosphatase Nonreceptor 11 (PTPN11), Carboxylesterase 1 (CES1), Recombinant Mitogen Activated Protein Kinase Kinase 2 (MAPKK2), MonoacylGLycerol Lipase (MGLL), and Translocator protein (TSPO).

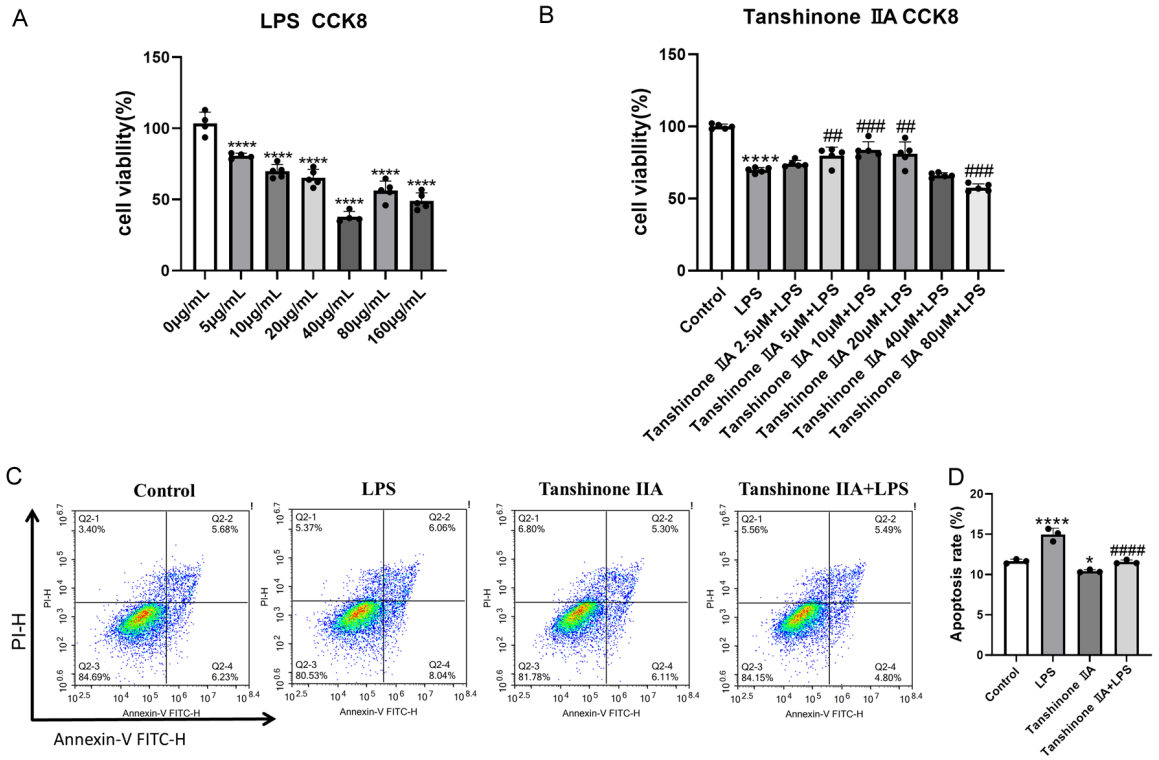

Figure 2. Tanshinone IIA treatment reduces LPS-induced HK2 cell apoptosis. A. Experimental exploration of LPS treatment concentration by CCK8 assay (compared with the 0 μg/mL group, ****P<0.0001; n=5); B. Experimental exploration of tanshinone IIA treatment concentration (compared with the Control group, ****P<0.0001; Compared with the LPS group, ##P<0.01; ###P<0.001; n=5); C, D. Flow cytometry detection of cell apoptosis (compared with the Control group, *P<0.05, ****P<0.0001; Compared with the LPS group, ####P<0.0001; n=3). LPS, lipopolysaccharide.

High throughput sequencing and qPCR validation of Differentially Expressed mRNAs in HK2 cells

HK2 cells in the LPS group and Tanshinone IIA + LPS group were subjected to high-throughput sequencing. As shown in **Figure 4A**, PAC results showed that the composition of three biological replicates in the two groups was similar, indicating good biological reproducibility of the cell samples. As shown in **Figure 4B**, the overall distribution of DEGs (LPS group vs. Tanshinone IIA + LPS group) is displayed using volcano plots. Compared with the LPS group, the Tanshinone IIA + LPS group exhibited 121 significantly upregulated genes and 65 significantly downregulated genes. A hierarchical clustering heatmap of DEGs is shown in **Figure 4C**, in which colors range from dark blue (low expression) to dark red (high expression), demonstrating clear gene expression differences between the two groups. GO enrichment analysis (**Figure 4D**) showed that DEGs were mainly enriched in biological processes related to RNA polymerase II - regulated transcription, apoptosis, and inflammatory responses; In terms of cellular composition, DEGs were mainly enriched in the cytoplasm, nucleus, and cell membrane; and for molecular function, DEGs were mainly associated with protein binding and DNA binding.

KEGG pathway enrichment (**Figure 4E**) showed that DEGs were primarily enriched in biological processes such as the p53 signaling pathway, cell cycle, and apoptosis. In response to external stimuli, DEGs were mainly concentrated in the mitogen activated protein kinase (MAPK) pathway, Forkhead box O (FoxO) pathway, and Phosphatidylinositol 3-kinase (PI3K)-Protein kinase B (AKT) pathway.

Based on sequencing results, six key DEGs were identified and subjected to qPCR validation. As shown in **Figure 4F-K**, compared with the LPS group, the expression levels of Growth arrest and DNA damage-45A

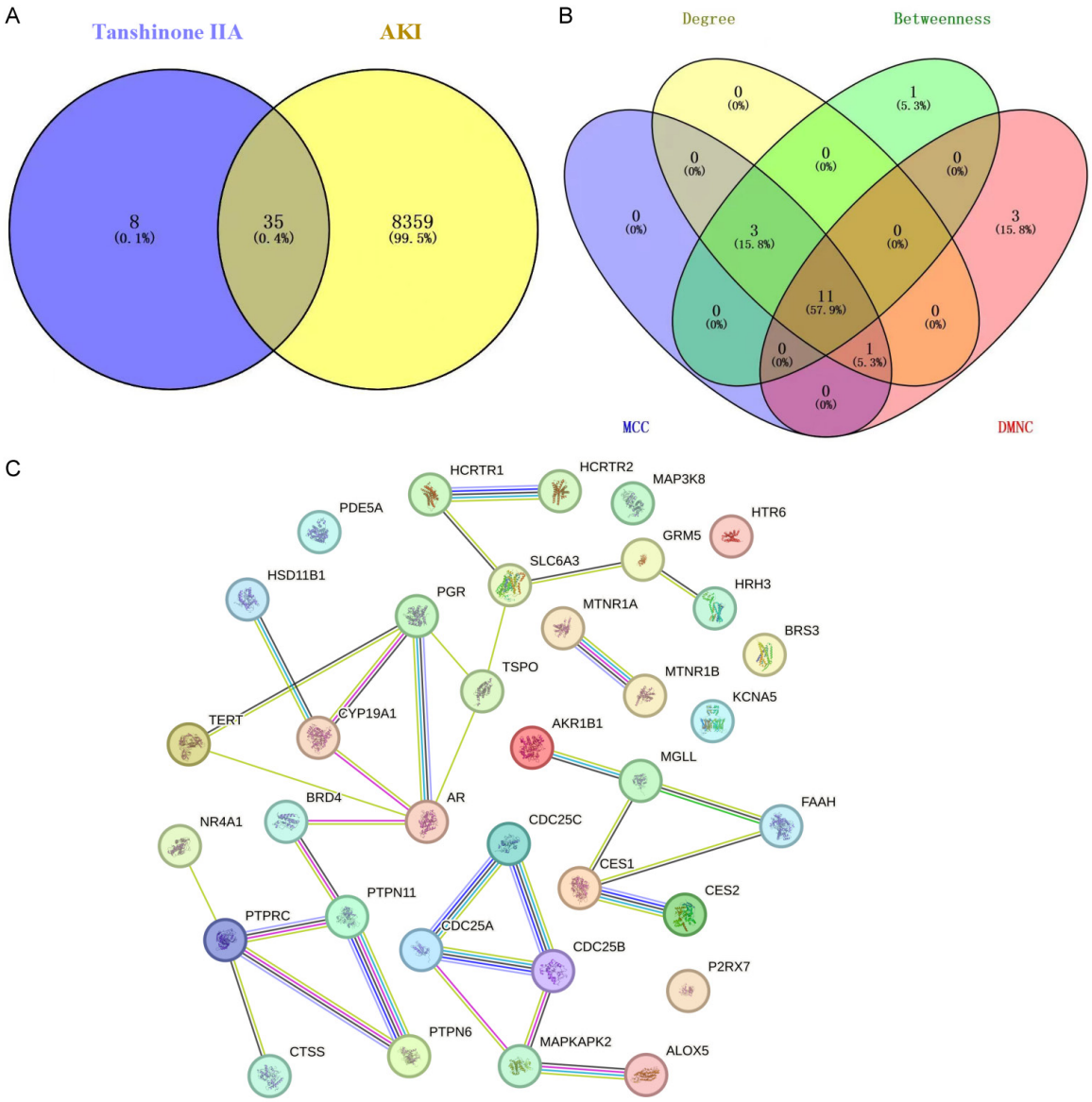

Figure 3. Prediction of Tanshinone IIA targets in AKI using network pharmacology. A. Thirty-five intersecting targets of Tanshinone IIA and AKI were obtained through the Venny 2.1.0 online platform; B. The core targets were obtained by selecting the top 15 using four algorithms: Degree, Betweenness, MCC, and DMNC; C. The PPI network was constructed through the String database.

(CADD45A), Ephrin A (EFNA), DNA Damage-inducible transcript 3 (DDIT3), and dual specificity phosphatase 10 (DUSP10) were significantly increased in the Tanshinone IIA + LPS group, and the expression levels of Heat shock protein family A member 1A (HSPA1A) and Egl-9 Family Hypoxia Inducible Factor 3 (EGLN3) were significantly decreased. The qPCR results were consistent with the high-throughput sequencing results.

Effects of tanshinone IIA on protein expression in model cells

Based on the high-throughput sequencing results of HK2 cells, it was speculated that the therapeutic effect of tanshinone IIA on SA-AKI may be achieved through the MAPK pathway, which is closely related to inflammation. To verify this hypothesis, western blot was used to detect the protein expression of DUSP10, p38,

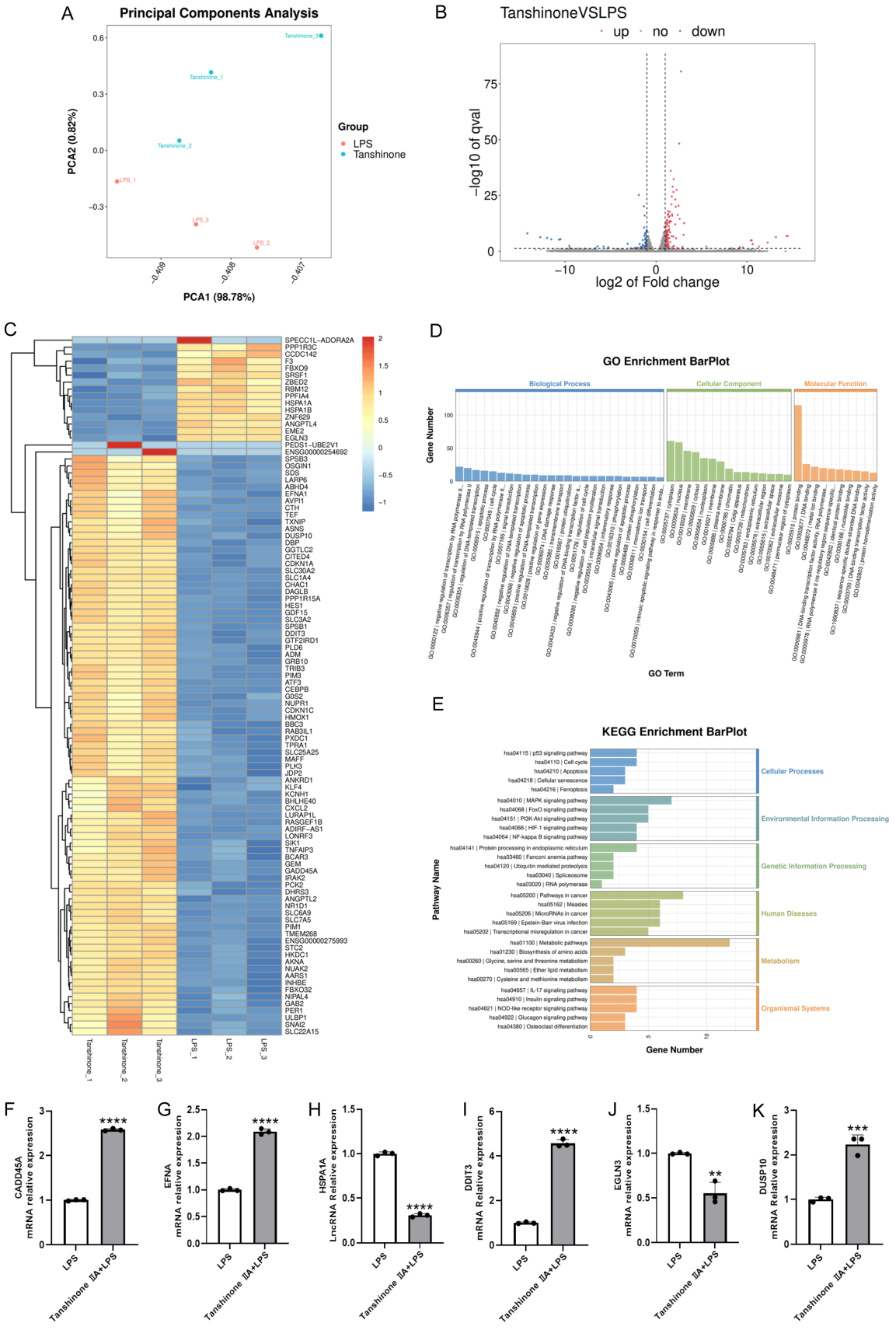
A
Principal Components Analysis
PCA2 (0.82%)
PCA1 (98.78%)
Group
LPS
Tanshinone
B
TanshinoneVSLPS
up
no
down
−log10 of qval
log2 of Fold change
C
D
GO Enrichment BarPlot
Biological Process
Cellular Component
Molecular Function
Gene Number
GO Term
E
KEGG Enrichment BarPlot
Cellular Processes
Environmental Information Processing
Genetic Information Processing
Human Diseases
Metabolism
Organismal Systems
Pathway Name
Gene Number
F
CADD45A mRNA relative expression
G
EFNA mRNA relative expression
H
HSPA1A LncRNA Relative expression
I
DDIT3 mRNA Relative expression
J
EGLN3 mRNA relative expression
K
DUSP10 mRNA Relative expression
LPS
Tanshinone ⅡA+LPS

Figure 4. High throughput sequencing and qPCR validation of Differentially Expressed mRNAs in HK2 cells (LPS group and Tanshinone IIA + LPS group). A. Principle components analysis (n=3); B. Volcano map of differentially expressed genes; C. Differential gene clustering heatmap; D. GO enrichment analysis of differentially expressed genes; E. KEGG enrichment analysis of differentially expressed genes; F-K. Relative expression levels of CADD45A, EFNA, HSPA1A, DDIT3, EGLN3, and DUSP10 mRNA (compared with LPS group, **P<0.01, ***P<0.001, ****P<0.0001; n=3). Notes: LPS, lipopolysaccharide; GO, Gene Ontology; KEGG, Kyoto Encyclopedia of Genes and Genomes; CADD45A, Growth arrest and DNA damage-45A; EFNA, Ephrin A; HSPA1A, Heat shock protein family A member 1A; DDIT3, DNA Damage-inducible transcript 3; EGLN3, Egl-9 Family Hypoxia Inducible Factor 3; DUSP10, dual specificity phosphatase 10.

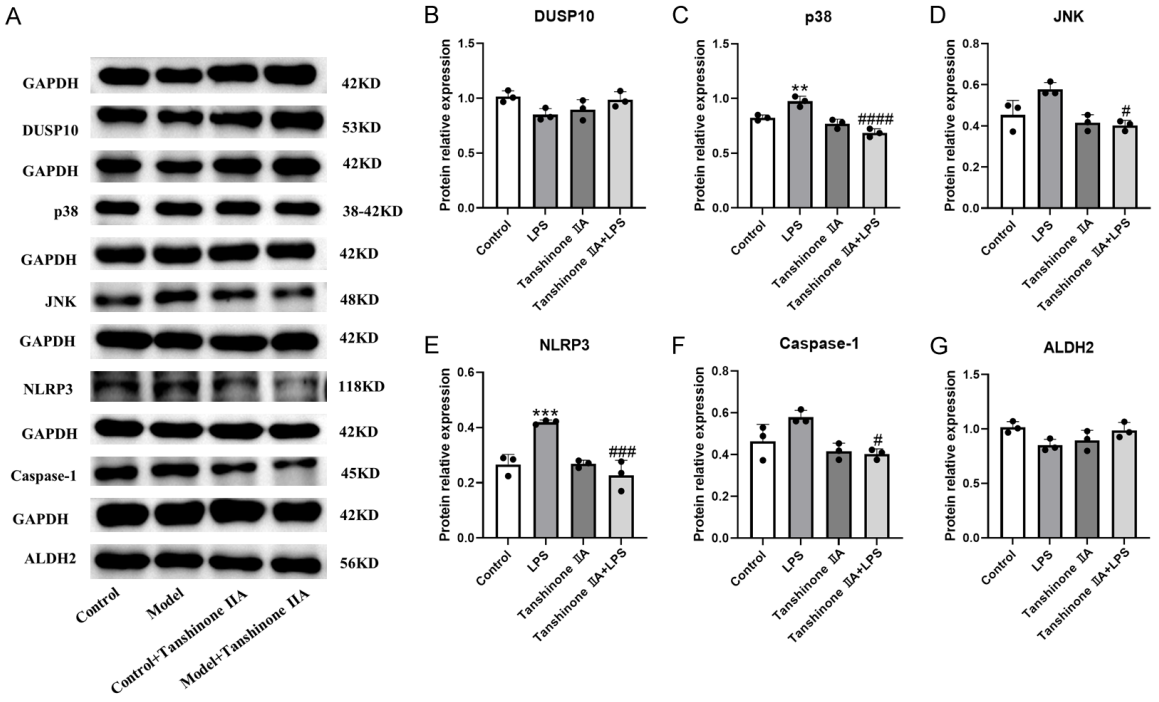

Figure 5. The expression of p38, JNK, NLRP3, and Caspase-1 proteins were down-regulated, while the expression of DUSP10 protein were upregulated after Tanshinone treatment in LPS-stimulated HK2 cells. A. Western blot results of HK2 cells; B-G. Statistical results of DUSP10, JNK, Caspase-1, and ALDH2 proteins in HK2 cells (compared with the Control group, **P<0.01, ***P<0.001; compared with the Model group, #P<0.05, ###P<0.001, ####P<0.0001; n=3). LPS, lipopolysaccharide; DUSP10, dual specificity phosphatase 10; JNK, c-Jun N-terminal kinase; NLRP3, nucleotide-binding oligomerization domain-like receptor protein 3; Caspase-1, cysteine aspartate specific protein 1; ALDH2, aldehyde dehydrogenase 2.

c-Jun N-terminal kinase (JNK), NLRP3, Cysteine aspartate specific protein 1 (Caspase-1), and ALDH2 in HK2 cells (**Figure 5A-G**). Compared with the Control group, the protein expression of p38 and NLRP3 was significantly increased in the LPS group, while the protein expression of JNK and Caspase-1 showed an upward trend (no significant difference). In contrast, protein expression of DUSP10 and ALDH2 showed a downward trend following LPS stimulation, but didn't reach statistical significance. Compared with the LPS group, the Tanshinone IIA + LPS group showed a significant decrease in the expression of p38, JNK, NLRP3, and Caspase-1 proteins, while the expression of DUSP10 and ALDH2 proteins showed an upward trend, although without statistical significance.

Effects of tanshinone IIA on protein expression in model mice

To validate the findings observed in cell experiments, we further examined the expression of key proteins in mouse kidney tissues. As shown in **Figure 6A-E**, IHC results showed that, compared with the Control group, the Model group demonstrated significantly increased expression of KIM-1 and NLRP3, and significantly decreased expression of DUSP10 and ALDH2. Following Tanshinone IIA pretreatment, the pro-

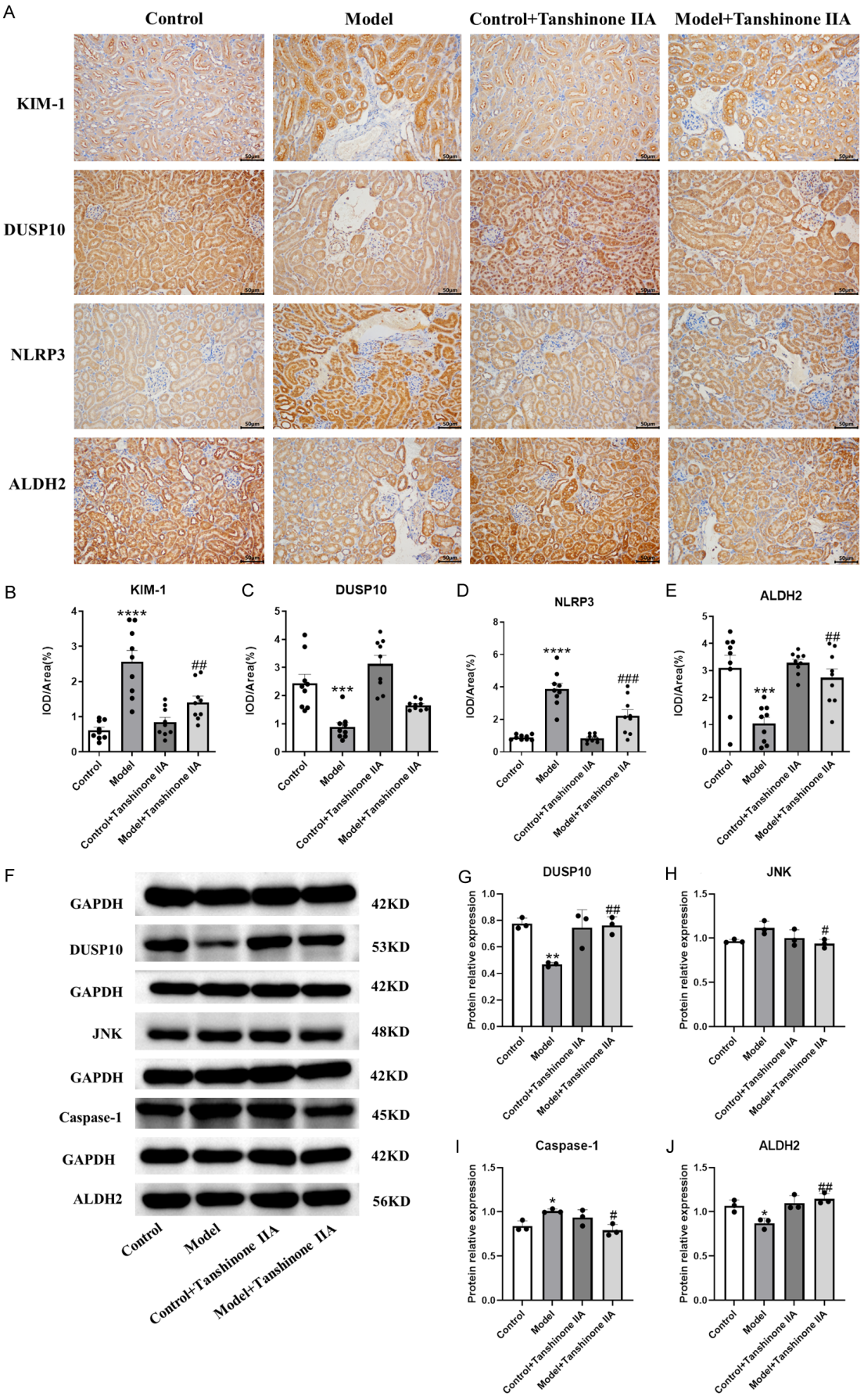
A
Control
Model
Control+Tanshinone IIA
Model+Tanshinone IIA
KIM-1
DUSP10
NLRP3
ALDH2
B
KIM-1
IOD/Area(%)
C
DUSP10
D
NLRP3
E
ALDH2
F
GAPDH
42KD
DUSP10
53KD
JNK
48KD
Caspase-1
45KD
G
DUSP10
H
JNK
I
Caspase-1
J
ALDH2
Protein relative expression

Figure 6. Tanshinone IIA pretreatment decreased the protein expression of JNK and Caspase-1 while it upregulated the expression of DUSP10 protein in SA-AKI mice. A. Immunohistochemical results of mouse kidney; B-E. Statistical results of KIM-1, DUSP10, NLRP3, and ALDH2 protein expression levels in mouse kidney. (compared with the Control group, ***P<0.001, ****P<0.0001; compared with the Model group, ##P<0.01, ###P<0.001; n=3); F. Western blot results of mouse kidney; G-J. The statistical results of DUSP10, JNK, Caspase-1, and ALDH2 proteins in the mouse kidney (compared with the Control group, *P<0.05, **P<0.01; Compared with the Model group, #P<0.05, ##P<0.01; n=3). Notes: DUSP10, dual specificity phosphatase 10; JNK, c-Jun N-terminal kinase; NLRP3, nucleotide-binding oligomerization domain-like receptor protein 3; Caspase-1, cysteine aspartate specific protein 1; ALDH2, aldehyde dehydrogenase 2; KIM-1, kidney injury molecule 1.

tein expression of KIM-1 and NLRP3 was significantly decreased while the ALDH2 protein expression was significantly increased; the expression of DUSP10 also showed an upward trend, but didn't reach statistical significance.

Similarly, WB results (**Figure 6F-J**) showed that compared with the Control group, the expression of JNK and Caspase-1 proteins was increased in the Model group, while the expression of DUSP10 and ALDH2 proteins was significantly decreased. Tanshinone IIA pretreatment significantly decreased the protein expression of JNK and Caspase-1 in the Model + Tanshinone IIA group, while the expression of DUSP10 and ALDH2 proteins was significantly increased. The above results were consistent with those in cell experiments.

Discussion

SA-AKI is a common yet severe complication in critically ill patients, with an incidence of about 30% in ICU. Depending on disease stage, the mortality rate ranges from 16.7% to 59.6% [27]. The high morbidity and mortality rates of SA-AKI pose significant challenges. The pathogenesis of SA-AKI is highly complex, involving inflammatory response, dysfunction of macro and micro blood vessels, cell apoptosis, necrosis, pyroptosis, ferroptosis, autophagy, and vesiculation etc. The interplay among these pathogenic processes [28] adds difficulty in elucidating the underlying mechanisms of SA-AKI. Tanshinone IIA, a bioactive compound extracted from Danshen, possesses anti-bacterial and anti-inflammatory properties. A study by Chen et al. has shown that tanshinone IIA can alleviate septic AKI in animal models [24].

In this study, SA-AKI was successfully induced in mice by intraperitoneal injection of LPS, as confirmed by significantly increased serum creatinine and urea nitrogen. Pre-administration of tanshinone IIA significantly decreased serum creatinine and urea nitrogen levels, alleviated renal injury, and reduced cell apoptosis. KIM-1 is a transmembrane protein mainly expressed in proximal renal tubular epithelial cells and is widely recognized as a biomarker of AKI. Upon acute injury, the expression of KIM-1 increases and is released into the renal tubules [29]. In addition, KIM-1 exerts anti-inflammatory effects, and various animal studies have demonstrated its protective role in attenuating AKI [30]. IHC results of mouse kidney tissue in this study showed that the expression level of KIM-1 was significantly increased in the model group, while its expression was significantly decreased in the model + tanshinone IIA group compared with model group. These findings confirm the successful establishment of the SA-AKI model and also prove that tanshinone IIA can mitigate renal injury.

To further investigate the molecular alterations associated with tanshinone IIA's protection against SA-AKI, HK2 cells were treated with LPS and tanshinone IIA, and high-throughput sequencing was performed to identify relevant DEGs. Results showed that 121 genes were significantly upregulated and 65 genes were significantly downregulated in the Tanshinone IIA + LPS group compared with the LPS group. GO and KEGG enrichment analysis identified 6 key DEGs (DDIT3, DUSP10, EFNA1, EGLN3, GADD45A, HSPA1A), which were selected to validate the high-throughput sequencing results through qPCR analysis. qPCR results showed that compared with the LPS group, the expression levels of CADD45A, EFNA, DDIT3 and DUSP10 were significantly upregulated in the tanshinone IIA + LPS group, while HSPA1A and EGLN3 were significantly downregulated, consistent with the results from high-throughput sequencing. Both high-throughput sequencing and qPCR results indicated a significant upregulation of DUSP10 following tanshinone IIA pre-administration. Given the proven regulatory role of DUSP10 in the MAPK signaling pathway, along with sequencing results, we hypoth-

esized that tanshinone IIA exerts therapeutic effects on SA-AKI by modulating the DUSP10-regulated MAPK signaling pathway. To verify this, further mechanistic experiments were performed.

The MAPK pathway is closely related to cell growth, inflammatory reactions and apoptosis. P38 mitogen activated protein kinase (p38 MAPK) and JNK are important members of the MAPK pathway. After activation, p38 migrates to the nucleus and regulates the inflammatory response by modulating transcription factor activity and cytokine synthesis [31]. It has been shown that LPS stimulation induces p38 activation of monocytes, neutrophils, and endothelial cells, leading to the release of a large amount of inflammatory mediators and acute inflammation [32]. p38 upregulates the expression of NLRP3 and pro-Interleukin-1beta (IL-1β) by activating transcription factors such as Nuclear factor kappa-B (NF-κB) or Activator Protein-1 (AP-1) [33]. The innate immune receptor NLRP3 inflammasome is a key factor in the SA-AKI inflammatory cascade, and NLRP3 can promote Caspase-1 activation and inflammatory cytokine expression, exacerbating the damage of the inflammatory response [13, 14]. JNK phosphorylation can activate downstream activator protein-1, which can regulate the expression of various interleukins and tumor necrosis factor, and promote an inflammatory response. In addition, JNK activation can activate B-cell lymphoma-2 (Bcl-2), participate in the release of apoptotic factors, and lead to Caspase activation and cell apoptosis [34]. JNK upregulates the expression of NLRP3 and pro-IL-1β by activating transcription factors (e.g., AP-1), thereby providing essential components for inflammasome activation [35]. The products of NLRP3 inflammasome activation (e.g., IL-1β) can further amplify p38 and JNK signaling, creating a pro-inflammatory feedback loop that exacerbates the inflammatory response [36]. Inhibiting the MAPK signaling pathway (with decreased expression of p38 and JNK) can hinder the inflammatory response and cell apoptosis in the renal tissue of hemorrhagic shock rats [37]. In our research, both animal and cell experiments showed that LPS-induced SA-AKI significantly increased the expression of p38, JNK, NLRP3, and Caspase-1 proteins. By pre-administration of tanshinone IIA, the expression of p38, JNK, NLRP3, and Caspase-1 proteins was significantly decreased, indicating that the SA-AKI inflammatory response may be caused by the activation of p38 and JNK in the MAPK signaling pathway. Tanshinone IIA can inhibit the activation of p38 and JNK in the MAPK signaling pathway, thus reducing the inflammatory response caused by SA-AKI.

It is still unclear which proteins tanshinone IIA may regulate to inhibit the MAPK signaling pathway and reduce the inflammatory response. DUSP10 can dephosphorylate the MAPK signaling pathway, with the strongest dephosphorylation activity towards p38 and JNK [38]. It has been shown that DUSP10 can inhibit the activation of activator protein-1 by dephosphorylating p38 and JNK, leading to a decrease in the expression of inflammatory factors and a weakening of the inflammatory response [39]. Elevated expression of DUSP10 can reduce any excessive inflammatory response. Many anti-inflammatory drugs have been identified to increase DUSP10 expression, such as compound Nepetoidin B, which upregulates DUSP10 expression in macrophages and inhibits p38 and JNK-dependent LPS-induced inflammatory response [40]. Therefore, DUSP10 may be a target for inhibiting the inflammatory response. In this study, the immunohistochemistry and western blot results from animal experiments showed that there is a significant decrease in DUSP10 protein expression in the model group. Compared with the model group, the DUSP10 protein expression was significantly increased in the model + tanshinone IIA group, and the same results were obtained in cell experiments. We found that tanshinone IIA can increase the expression of DUSP10, and inhibit p38 and JNK-dependent LPS-induced inflammatory responses, suggesting that tanshinone IIA exerts anti-inflammatory and anti-apoptotic effects through the DUSP10/JNK/p38/NLRP3 signaling pathway. In addition, this study provided another possible mechanism for the treatment of SA-AKI with tanshinone IIA.

During the SA-AKI inflammatory response, oxidative stress occurs, producing a large amount of ROS. Meanwhile, oxidative metabolism produces a large amount of aldehydes, causing oxidative damage to cells. Aldehyde dehydrogenase 2 can reduce the accumulation of aldehydes and weaken their toxicity [41]. The immunohistochemistry and western blot results from

the animal experiments showed a significant decrease in ALDH2 protein expression in the model group. Compared with the model group, the ALDH2 protein expression was significantly increased in the model + tanshinone IIA group, and the same results were obtained in cell experiments. However, ALDH2 was not detected in the differentially expressed genes by high-throughput sequencing. How tanshinone IIA regulates ALDH2 will be investigated in subsequent experiments.

Conclusion

Tanshinone IIA may regulate the JNK/P38/NLRP3 pathway in SA-AKI by upregulating DUSP10, thereby exerting a protective effect by reducing inflammation and cell apoptosis, and preventing SA-AKI.

Acknowledgements

This work was supported by the National Natural Science Foundation of China (No. 820-60140 and No. 81660129).

Disclosure of conflict of interest

None.

Address correspondence to: Jinlei Lv, Department of Nephrology, The 1st Affiliated Hospital, Jiangxi Medical College, Nanchang University, Institute of Molecular Immunology for Kidney Disease of Nanchang University, No. 17 Yongwai Zheng Street, Donghu District, Nanchang 330000, Jiangxi, China. Tel: +86-0791-88693235; E-mail: lvjinlei97@163.com

References

[1] Seymour CW, Liu VX, Iwashyna TJ, Brunkhorst FM, Rea TD, Scherag A, Rubenfeld G, Kahn JM, Shankar-Hari M, Singer M, Deutschman CS, Escobar GJ and Angus DC. Assessment of clinical criteria for sepsis: for the third international consensus definitions for sepsis and septic shock (sepsis-3). JAMA 2016; 315: 762-774.

[2] Zarbock A, Nadim MK, Pickkers P, Gomez H, Bell S, Joannidis M, Kashani K, Koyner JL, Pannu N, Meersch M, Reis T, Rimmelé T, Bagshaw SM, Bellomo R, Cantaluppi V, Deep A, De Rosa S, Perez-Fernandez X, Husain-Syed F, Kane-Gill SL, Kelly Y, Mehta RL, Murray PT, Ostermann M, Prowle J, Ricci Z, See EJ, Schneider A, Soranno DE, Tolwani A, Villa G, Ronco C and Forni LG. Sepsis-associated acute kidney injury: consensus report of the 28th Acute Disease Quality Initiative workgroup. Nat Rev Nephrol 2023; 19: 401-417.

[3] Kellum JA, Chawla LS, Keener C, Singbartl K, Palevsky PM, Pike FL, Yealy DM, Huang DT and Angus DC. The effects of alternative resuscitation strategies on acute kidney injury in patients with septic shock. Am J Respir Crit Care Med 2016; 193: 281-287.

[4] Formeck CL, Feldman R, Althouse AD and Kellum JA. Risk and timing of De Novo sepsis in critically ill children after acute kidney injury. Kidney360 2023; 4: 308-315.

[5] Hoste EA, Bagshaw SM, Bellomo R, Cely CM, Colman R, Cruz DN, Edipidis K, Forni LG, Gomersall CD, Govil D, Honoré PM, Joannes-Boyau O, Joannidis M, Korhonen AM, Lavrentieva A, Mehta RL, Palevsky P, Roessler E, Ronco C, Uchino S, Vazquez JA, Vidal Andrade E, Webb S and Kellum JA. Epidemiology of acute kidney injury in critically ill patients: the multinational AKI-EPI study. Intensive Care Med 2015; 41: 1411-1423.

[6] Tejera D, Varela F, Acosta D, Figueroa S, Benencio S, Verdaguer C, Bertullo M, Verga F and Cancela M. Epidemiology of acute kidney injury and chronic kidney disease in the intensive care unit. Rev Bras Ter Intensiva 2017; 29: 444-452.

[7] Chua HR, Wong WK, Ong VH, Agrawal D, Vathsala A, Tay HM and Mukhopadhyay A. Extended mortality and chronic kidney disease after septic acute kidney injury. J Intensive Care Med 2020; 35: 527-535.

[8] Pinheiro KHE, Azêdo FA, Areco KCN and Laranja SMR. Risk factors and mortality in patients with sepsis, septic and non septic acute kidney injury in ICU. J Bras Nefrol 2019; 41: 462-471.

[9] Adhikari NK, Fowler RA, Bhagwanjee S and Rubenfeld GD. Critical care and the global burden of critical illness in adults. Lancet 2010; 376: 1339-1346.

[10] Yang M, Lu L, Kang Z, Ma T and Wang Y. Overexpressed CD39 mitigates sepsis-induced kidney epithelial cell injury via suppressing the activation of NLR family pyrin domain containing 3. Int J Mol Med 2019; 44: 1707-1718.

[11] Zhang J, Qi M, Ma L and Liu D. Research progress on biomarkers of sepsis-associated acute kidney injury. Zhonghua Wei Zhong Bing Ji Jiu Yi Xue 2024; 36: 1216-1220.

[12] Ludes PO, De Roquetaillade C, Chousterman BG, Pottecher J and Mebazaa A. Role of damage-associated molecular patterns in septic acute kidney injury, from injury to recovery. Front Immunol 2021; 12: 606622.

[13] Gao Y, Dai X, Li Y, Li G, Lin X, Ai C, Cao Y, Li T and Lin B. Role of Parkin-mediated mitophagy in the protective effect of polydatin in sepsis-

induced acute kidney injury. J Transl Med 2020; 18: 114.
[14] Huang G, Bao J, Shao X, Zhou W, Wu B, Ni Z and Wang L. Inhibiting pannexin-1 alleviates sepsis-induced acute kidney injury via decreasing NLRP3 inflammasome activation and cell apoptosis. Life Sci 2020; 254: 117791.
[15] Fry DE. Sepsis, systemic inflammatory response, and multiple organ dysfunction: the mystery continues. Am Surg 2012; 78: 1-8.
[16] Dellepiane S, Marengo M and Cantaluppi V. Detrimental cross-talk between sepsis and acute kidney injury: new pathogenic mechanisms, early biomarkers and targeted therapies. Crit Care 2016; 20: 61.
[17] Dou JY, Zhang M, Cen H, Chen YQ, Wu YF, Lu F, Zhou J, Liu XS and Gu YY. Salvia miltiorrhiza Bunge (Danshen) and bioactive compound tanshinone IIA alleviates cisplatin-induced acute kidney injury through regulating PXR/NF-κB signaling. Front Pharmacol 2022; 13: 860383.
[18] Yang L, Huang X, Wang Z, Guo Z, Ma C, Dong L, Luo Y, Hu X, Chen F and Li D. Research progress on the pharmacological properties of active ingredients from Salvia miltiorrhiza: a review. Phytomedicine 2025; 148: 157272.
[19] MEIm XD, Cao YF, Che YY, Li J, Shang ZP, Zhao WJ, Qiao YJ and Zhang JY. Danshen: a phytochemical and pharmacological overview. Chin J Nat Med 2019; 17: 59-80.
[20] Du S, Yao Q, Tan P, Xie G, Ren C, Sun Q, Zhang X, Zheng R, Yang K, Yuan Y and Yuan Q. Protective effect of tanshinone IIA against radiation-induced ototoxicity in HEI-OC1 cells. Oncol Lett 2013; 6: 901-906.
[21] Wang XX, Yang JX, Pan YY and Zhang YF. Protective effects of tanshinone IIA on endothelial progenitor cells injured by tumor necrosis factor-α. Mol Med Rep 2015; 12: 4055-4062.
[22] Wu X, Liu L, Xie H, Liao J, Zhou X, Wan J, Yu K, Li J and Zhang Y. Tanshinone IIA prevents uric acid nephropathy in rats through NF-κB inhibition. Planta Med 2012; 78: 866-873.
[23] Kim SK, Jung KH and Lee BC. Protective effect of Tanshinone IIA on the early stage of experimental diabetic nephropathy. Biol Pharm Bull 2009; 32: 220-224.
[24] Tai H, Cui XZ, He J, Lan ZM, Li SM, Li LB, Yao SC, Jiang XL, Meng XS and Kuang JS. Renoprotective effect of Tanshinone IIA against kidney injury induced by ischemia-reperfusion in obese rats. Aging (Albany NY) 2022; 14: 8302-8320.
[25] Jiang C, Zhu W, Shao Q, Yan X, Jin B, Zhang M and Xu B. Tanshinone IIA protects against folic acid-induced acute kidney injury. Am J Chin Med 2016; 44: 737-753.
[26] Min W and Zhulan X. Effect of acid II A injection combined with rhubarb preparation on oxidative stress apoptosis in mice with acute kidney injury. Tianjin Pharmaceutical 2022; 34: 7-10.
[27] Fan T, Song S, Li H, Bai Y, Chen Y and Cheng B. Knowledge graph characteristics of sepsis research based on scientometric study. Zhonghua Wei Zhong Bing Ji Jiu Yi Xue 2021; 33: 433-437.
[28] Kounatidis D, Vallianou NG, Psallida S, Panagopoulos F, Margellou E, Tsilingiris D, Karampela I, Stratigou T and Dalamaga M. Sepsis-associated acute kidney injury: where are we now? Medicina (Kaunas) 2024; 60: 434
[29] Kuchroo VK, Meyers JH, Umetsu DT and Dekruyff RH. TIM family of genes in immunity and tolerance. Adv Immunol 2006; 91: 227-249.
[30] Yang L, Brooks CR, Xiao S, Sabbisetti V, Yeung MY, Hsiao LL, Ichimura T, Kuchroo V and Bonventre JV. KIM-1-mediated phagocytosis reduces acute injury to the kidney. J Clin Invest 2015; 125: 1620-1636.
[31] Klein AM, Zaganjor E and Cobb MH. Chromatin-tethered MAPKs. Curr Opin Cell Biol 2013; 25: 272-277.
[32] Jiang Y and Gong XW. Regulation of inflammatory responses by MAPK signal transduction pathways. Sheng Li Xue Bao 2000; 52: 267-271.
[33] Bauernfeind FG, Horvath G, Stutz A, Alnemri ES, Macdonald K, Speert D, Fernandes-Alnemri T, Wu J, Monks BG, Fitzgerald KA, Hornung V and Latz E. Cutting edge: NF-kappaB activating pattern recognition and cytokine receptors license NLRP3 inflammasome activation by regulating NLRP3 expression. J Immunol 2009; 183: 787-791.
[34] Takano T, Fiore S, Maddox JF, Brady HR, Petasis NA and Serhan CN. Aspirin-triggered 15-epi-lipoxin A4 (LXA4) and LXA4 stable analogues are potent inhibitors of acute inflammation: evidence for anti-inflammatory receptors. J Exp Med 1997; 185: 1693-1704.
[35] Gross O, Yazdi AS, Thomas CJ, Masin M, Heinz LX, Guarda G, Quadroni M, Drexler SK and Tschopp J. Inflammasome activators induce interleukin-1α secretion via distinct pathways with differential requirement for the protease function of caspase-1. Immunity 2012; 36: 388-400.
[36] Swanson KV, Deng M and Ting JP. The NLRP3 inflammasome: molecular activation and regulation to therapeutics. Nat Rev Immunol 2019; 19: 477-489.
[37] Chang SY, Sun RQ, Feng M, Li YX, Wang HL and Xu YM. BML-111 inhibits the inflammatory response and apoptosis of renal tissue in rats with hemorrhagic shock by inhibiting the MAPK pathway. Eur Rev Med Pharmacol Sci 2018; 22: 3439-3447.

[38] Theodosiou A, Smith A, Gillieron C, Arkinstall S and Ashworth A. MKP5, a new member of the MAP kinase phosphatase family, which selectively dephosphorylates stress-activated kinases. Oncogene 1999; 18: 6981-6988.
[39] Jiménez-Martínez M, Stamatakis K and Fresno M. The dual-specificity phosphatase 10 (DUSP10): its role in cancer, inflammation, and immunity. Int J Mol Sci 2019; 20: 1626.
[40] Wu X, Gao H, Sun W, Yu J, Hu H, Xu Q and Chen X. Nepetoidin B, a natural product, inhibits LPS-stimulated nitric oxide production via modulation of iNOS mediated by NF-κB/MKP-5 pathways. Phytother Res 2017; 31: 1072-1077.
[41] Chen CH, Budas GR, Churchill EN, Disatnik MH, Hurley TD and Mochly-Rosen D. Activation of aldehyde dehydrogenase-2 reduces ischemic damage to the heart. Science 2008; 321: 1493-1495.